A Near-Infrared Transient Absorption Study of the Excited-State Dynamics of the Carotenoid Spirilloxanthin in Solution and in the LH1 Complex of *Rhodospirillum rubrum*

Emmanouil Papagiannakis,* Ivo H. M. van Stokkum, and Rienk van Grondelle

Department of Biophysics, Division of Physics and Astronomy, Vrije Universiteit, De Boelelaan 1081, 1081 HV Amsterdam, The Netherlands

Robert A. Niederman

Department of Molecular Biology and Biochemistry, Rutgers University, Piscataway, New Jersey 08854

Donatas Zigmantas, Villy Sundström, and Tomáš Polívka

Department of Chemical Physics, Lund University, P.O. Box 124, 22100 Lund, Sweden

Received: April 8, 2003; In Final Form: July 31, 2003

The spectroscopic properties of spirilloxanthin in an *n*-hexane solution and bound to the core light-harvesting (LH1) complex of *Rhodospirillum rubrum* were studied by near-infrared ultrafast transient absorption spectroscopy. Global analysis of the kinetic traces measured after excitation of spirilloxanthin to the S_2 ($1B_u^+$) state enabled us to estimate the species-associated difference spectra that correspond to the excited-state absorption signals originating from the S_1 ($2A_g^-$) and S_2 states. Analysis of the absorption originating from the S_2 state has provided further insight into the characterization of the spirilloxanthin excited states, while by analyzing the profile of the S_1-S_2 transition, we place the energy of the S_1 state of *all-trans*-spirilloxanthin at 11 500 cm^{-1}, both in solution and in the LH1 complex. This low value excludes excitation energy transfer from the S_1 state of spirilloxanthin to bacteriochlorophyll in the LH1 complex of *Rs. rubrum* and explains the observed low energy transfer efficiency from spirilloxanthin to bacteriochlorophyll in that complex. Our results indicate that the S* state of spirilloxanthin, which was recently found both in solution and in the LH1 complex (Gradinaru, C. C., *et al*. *Proc. Natl. Acad. Sci. U.S.A.* **2001**, *98*, 2364), does not exhibit detectable spectral features in the near-infrared region.

Introduction

The excited-state properties of carotenoids are largely determined by their polyene backbone and play an important role in the functional photochemistry of photosynthetic organisms.[1,2] Hitherto, at least two excited singlet states have been included in the description of this function of carotenoids: the S_2 ($1B_u^+$ in C_{2h} symmetry group notation applicable for polyenes) state that accounts for the strong absorption of blue-green light and the S_1 ($2A_g^-$) state, which is inaccessible from the ground state S_0 ($1A_g^-$) by one-photon absorption. The existence of other singlet states, such as the $1B_u^-$ state and the $3A_g^-$ state, has been theoretically predicted for polyenes[3] and reported recently by spectroscopic measurements on various carotenoids.[4,5] In addition to the theoretically predicted singlet states, a new state denoted S*, whose symmetry properties remain to be identified, was recently revealed in some carotenoids.[6−8] Since these "dark" states are located between the S_1 and S_2 states, it has been suggested that they play an important role in the relaxation pathways of carotenoid molecules[4−7] and even in mediating excitation energy transfer (EET) to bacteriochlorophyll *a* (BChl).[7] Absorption of light promotes carotenoids to the S_2 state, which rapidly relaxes to populate the lower singlet states on the time scale of 50−300 fs. Subsequently, the S_1 state decays by internal conversion (IC) to the ground state on the picosecond time scale. The dependence of the S_1 lifetime on the conjugation length has been clearly demonstrated using a series of spheroidene analogues having different conjugation lengths, which exhibit a variation of the S_1 lifetime from 400 ps ($N = 7$) to 1.1 ps ($N = 13$).[9] Consequently, according to the energy gap law,[10] carotenoids with more than 10 C=C bonds are expected to have a rather low S_1 energy compared to the energy of the BChl acceptor states in bacterial light-harvesting (LH) complexes, making the S_1 state inefficient in, or incapable of, energy transfer. As shown for a number of photosynthetic light-harvesting complexes,[2,11] the lifetimes and the energies of the lowest excited states of carotenoids are crucial parameters governing efficiencies of carotenoid−BChl energy transfer.

Spirilloxanthin, so far the most unsaturated carotenoid known to be involved in photosynthetic light harvesting, has 13 double bonds and is found in the LH complexes of various photosynthetic bacteria, serving as both a light-harvesting and photoprotective pigment. It is the sole carotenoid found in the LH apparatus of *Rhodospirillum* (*Rs.*) *rubrum*,[12] which is relatively simple in that it comprises only one type of antenna, the so-called LH1 complex, which surrounds the reaction center protein and most likely consists of a ring-like array of 16 $\alpha\beta$-polypeptide subunits, each subunit binding a pair of BChls and one spirilloxanthin.[13] As a consequence of its extended conjugation, the S_1 state of spirilloxanthin is short-lived and decays to the ground state in 1.4 ps both in solution and in the LH1 complex of *Rs. rubrum*.[6] This indicates that no energy transfer

* To whom correspondence should be addressed. Fax: +31-20-4447999. E-mail: papagian@nat.vu.nl.

10.1021/jp034931j CCC: $25.00
Published on Web 09/03/2003

occurs from the spirilloxanthin S_1 state to the Q_y state of BChl, resulting in the low total efficiency of spirilloxanthin−BChl energy transfer of ∼30%.[14] Interestingly, spirilloxanthin is one of the few carotenoids[15] in which the newly found S* state appears also in solution. This state was identified by its excited-state absorption (ESA) in the visible region, which has a spectral profile and a lifetime clearly distinct from that of the S_1 state and is populated directly from the S_2 state, in parallel with the S_1 state.[6] In the LH1 complex of *Rs. rubrum*, S* is on the pathway of ultrafast carotenoid triplet formation via the singlet-fission mechanism, while in solution it decays to the ground state in 5 ps without detectable triplet formation. Recently, the S* state was also identified in a different antenna, the LH2 complex of *Rhodobacter* (*Rb.*) *sphaeroides* which binds the carotenoid spheroidene.[7] In contrast to spirilloxanthin, the S* state is not observed in spheroidene in solution.[15]

These properties of spirilloxanthin and the current interest in hitherto unobserved carotenoid states in bacterial LH complexes encouraged us to perform transient absorption measurements of spirilloxanthin in the near-infrared (near-IR) spectral region, where the optically allowed S_1-S_2 transition of carotenoids can be detected. This experimental approach has been useful in obtaining information about the energy of the S_1 state of carotenoids, both in solution and in LH complexes.[16−20] Furthermore, the application of this method in studying the dynamics of spheroidene in the LH2 complex of *Rb. sphaeroides* revealed an additional spectral feature, which was attributed to the ultrafast formation of a spheroidene radical in the LH2 complex.[18] This radical decays with almost the same time constant as the S* state of spheroidene in the same complex;[7] hence, it was hypothesized that these two species may be of the same origin.[18] Here we report the near-IR transient absorption study of the carotenoid spirilloxanthin after excitation to the S_2 state, both in an *n*-hexane solution and in the LH1 complex of *Rs. rubrum*. In both environments, an intense and broad ESA which appears upon excitation decays on a 100 fs time scale, to be followed by a weak ESA with the dynamics of S_1 and a profile characteristic of the S_1-S_2 transition. Study of the temporal and spectral characteristics of these features allows us to further characterize the relaxation processes that follow excitation to the S_2 state and to determine the energy of the S_1 state of spirilloxanthin, confirming that it is too low to participate in energy transfer to BChl in the LH1 complex. Notably, no features related to the S* state or a spirilloxanthin radical have been observed.

Materials and Methods

Sample Preparation. Spirilloxanthin was isolated from stationary-phase *Rs. rubrum* cells in an effort to limit the presence of spirilloxanthin precursors.[21] After extraction and chromatography on an alumina column as described by Komori *et al*.,[22] purified spirilloxanthin was dissolved in *n*-hexane to an absorbance of 0.16 mm^{-1} at the excitation wavelength of 520 nm. Isolated LH1 complexes devoid of reaction centers were obtained as described by Picorel *et al*.[12] An HPLC assay indicated that exclusively BChl and spirilloxanthin were present in this preparation. The isolated LH1 complex of *Rs. rubrum* is very sensitive to the presence of detergent in the buffer. We observed that an LDAO concentration of ∼0.1% was enough to cause significant spectral alterations to the complex within a few minutes, monitored by the decrease in absorption at 880 nm and the rise of the free BChl peak at 770 nm. Therefore, in our measurements, the LH1 complex was suspended in an essentially detergent-free state in D_2O-Tris buffer (pH 7.5), resulting in associated LH1 oligomers rather than in individual protomers. The use of D_2O instead of H_2O is necessary to avoid the significant absorption of H_2O in the near-IR region. The absorbance of the sample was 0.1 mm^{-1} at the 540 nm excitation wavelength. The samples were kept frozen at −40 °C in the dark and thawed only before the measurements.

Ultrafast Near-IR Spectroscopy. The experimental setup was described in detail previously.[17] In brief, a 5 kHz amplified Ti: sapphire laser system (Tsunami-Spitfire, Spectra Physics) was used to pump two computer-controlled optical parametric amplifiers (TOPAS, Light Conversion). One TOPAS provided pulses that were used for excitation of the samples, and was tuned to either 520 or 540 nm to excite the lowest vibronic level of the S_2 state of spirilloxanthin in *n*-hexane or LH1, respectively. The second TOPAS provided probe pulses in the range of 880−1820 nm. The pulses were ∼160 fs long and were focused to a spot 200 μm in diameter, while the energy used for excitation was kept moderately low at 20 nJ per pulse. The relative delay between pump and probe pulses was controlled by an optical delay line, and their mutual polarization was set to the magic angle (54.7°). A 2-mm path spinning cell was used for the measurements to limit exposure of the sample to multiple laser shots. Absorption measurements before, during, and after the experiments showed no UV absorption that could be attributed to degradation products, indicating that no sample degradation occurred, although formation of isomers during the course of measurements was unavoidable (see below). A large number of kinetic traces were obtained, each consisting typically of 150 delay points. Approximately 50 000 shots were averaged per delay point to achieve a sufficient signal-to-noise ratio.

Global Analysis. All the kinetic traces were globally analyzed[23] in an effort to estimate the decay constants required for a satisfactory fit, and subsequently, the appropriate model, sequential or branched, was applied. In this way, the data can be described by a set of species-associated difference spectra (SADS), each of them having a discreet lifetime. In the basic descriptive model, SADS appear sequentially (i.e., 1 → 2 → 3 → 4), and each of them evolves with an increasingly longer lifetime into the next. With this process, all the spectral and transient evolution in the data is described optimally, leading to a clear picture of the events that take place. It has to be noted, however, that in the basic sequential description, the SADS are not necessarily associated with pure excited molecular species and potentially portray the coexistence of different species. In more complicated cases, like in LH complexes, it has been shown that target analysis,[24] which involves the application of a specific, branched modeling scheme, can lead to disentanglement of different, parallel relaxation pathways and the estimation of SADS corresponding to the pure excited states.[6,7] The fitting procedure involves deconvolution of the instrument response function which for these experiments was fitted to a Gaussian of ∼230 fs (fwhm), varying slightly in different wavelength regions.

Results

Spirilloxanthin in Solution. The absorption spectrum of spirilloxanthin in *n*-hexane (Figure 1) shows the characteristic three-peak structure with the lowest 0−0 vibrational transition located at 522 nm. The position of this peak, which is blue-shifted compared to the reported value of 526 nm[25−28] observed in our freshly column-purified samples, as well as the presence of absorption bands around 380 nm indicate that in addition to *all-trans*-spirilloxanthin, some *cis* isomer is also present. However, the small amplitude of the 380 nm bands indicates

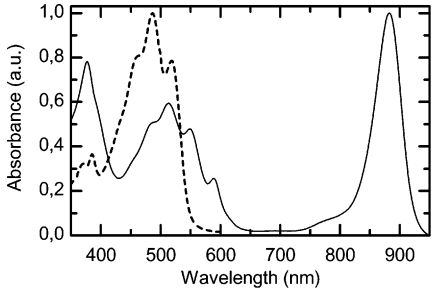

Figure 1. Steady-state absorption spectra of spirilloxanthin in *n*-hexane (- - -) and the LH1 complex of *Rs. rubrum* (—).

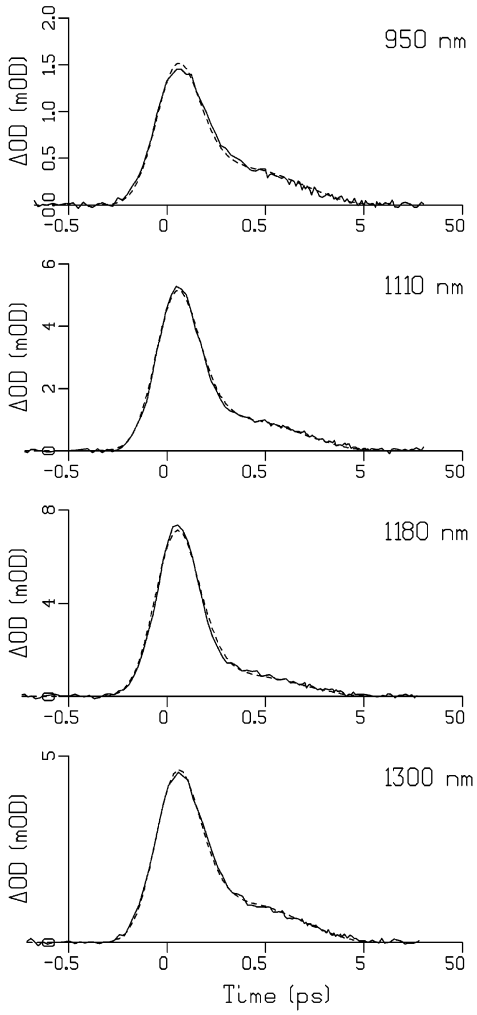

Figure 2. Characteristic kinetic traces measured on spirilloxanthin in *n*-hexane after excitation of the lowest vibrational band of the S_2 state at 520 nm. The dashed lines represent the fits. Note that the scale is logarithmic above 0.5 ps.

that the predominant species in the solution is *all-trans*-spirilloxanthin, since for *cis*-spirilloxanthin, the amplitude of the *cis* peak around 380 nm is similar to that of the main bands.[28] The existence of conformations other than the *all-trans* form in solution is anticipated, because spirilloxanthin isomerizes spontaneously on a time scale of minutes.[26] Spirilloxanthin was excited to its S_2 state with 520 nm laser pulses, and kinetic traces were measured at 55 probing wavelengths spanning the spectral region from 880 to 1620 nm, where the S_1-S_2 transition is expected to appear. All the recorded traces were analyzed simultaneously, and two decay components were enough to obtain a globally excellent fit (Figure 2). The corresponding

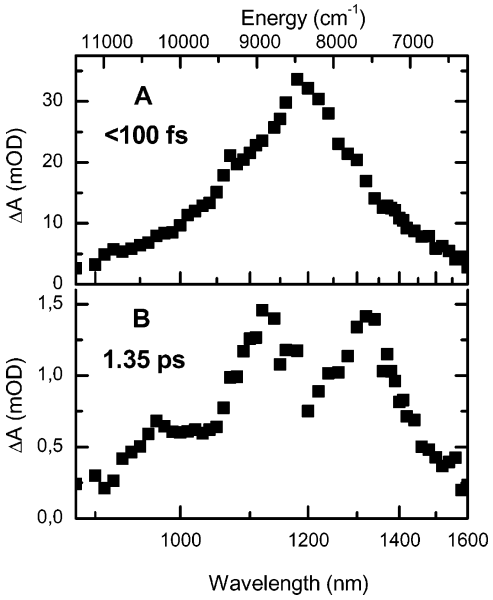

Figure 3. SADS and associated lifetimes characterizing the spectral evolution of the transient absorption of spirilloxanthin in *n*-hexane in the near-IR region after excitation at 520 nm.

SADS (Figure 3) show clear spectral shapes enabling the identification of the spectral and temporal evolution.

Upon excitation, we observe an intense structureless ESA band centered at 1180 nm (Figure 3A). With a lifetime of <100 fs (instrument response-limited), this feature evolves into a low-amplitude ESA, which has a lifetime of 1.35 ps. The structure of this SADS (Figure 3B) exhibits the clear three-peak shape expected for the S_1-S_2 absorption.[17] The first decay component can be firmly attributed to the depopulation of the S_2 state, which has an intense ESA to a high-energy state in this spectral region,[17,29] most likely to a state of A_g^- symmetry. The SADS that corresponds to this component (Figure 3A) is very broad and peaks at 1180 nm (8475 cm^{-1}). If the S_2-state energy is taken into account, the higher A_g^--state energy can be estimated to be at approximately 27 500 cm^{-1}. It is noteworthy that with our limited time resolution we do not observe any signs of a spectral evolution taking place on the very fast time scale, such as the one interpreted by Koyama and co-workers[4] as a signature of an electronic state interfering with the IC from S_2 to S_1. The lifetime of the second SADS (Figure 3B) is 1.35 ± 0.2 ps, matching the lifetime of 1.4 ps for the S_1 state of spirilloxanthin as determined by probing the decay of its ESA in the visible spectral range.[6] This indicates that this SADS, which has pronounced structure, indeed reflects the transitions between S_1 and the different vibrational levels of S_2. The peaks attributed to the 0−2, 0−1, and 0−0 vibrational bands of the S_1-S_2 transition are located at 970, 1120, and 1320 nm (10 310, 8930, and 7575 cm^{-1}), respectively. The energy gaps between vibrational peaks (1380 and 1355 cm^{-1}) are close to those observed for the S_2 vibrational sublevels as calculated from the ground-state absorption spectrum (1310 and 1295 cm^{-1}).

There is no indication of an additional sub-picosecond component that could be associated with the vibrational cooling of the S_1 state, which has been observed in other experiments on a number of carotenoids, both in the near-IR region[17] and in the visible region.[30,31] In spirilloxanthin, the relaxation of the S_1 state is not so pronounced, occurs within 200 fs,[15] and most probably is not detectable within the signal-to-noise ratio of these experiments. Furthermore, no slow decay component that could directly be related to the occurrence of the S* state is observed. This state was identified by its ESA in the visible

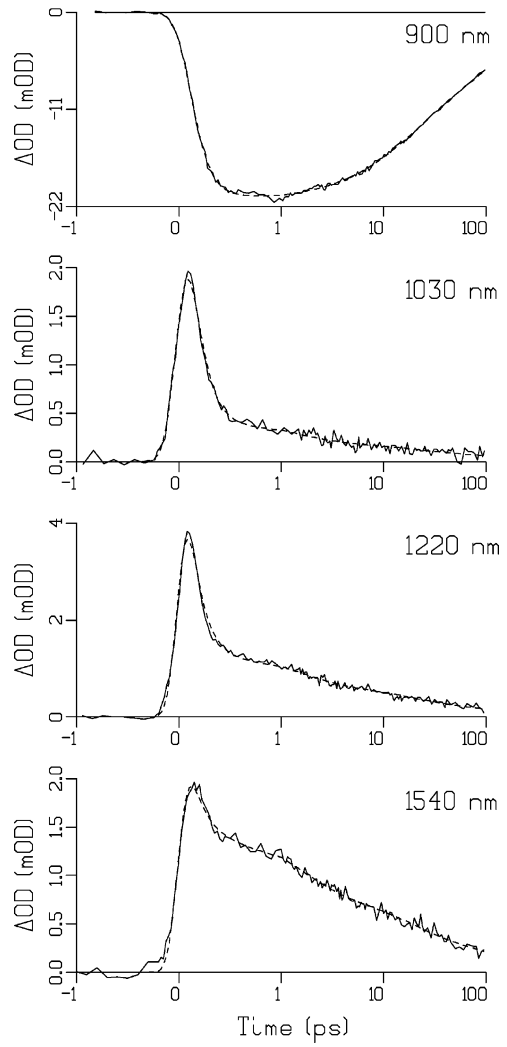

Figure 4. Characteristic kinetic traces measured on the LH1 complex of *Rs. rubrum* after excitation of the lowest vibrational band of the S_2 state of spirilloxanthin at 540 nm. The dashed lines represent the fits. Note that the scale is logarithmic above 1 ps.

region and has a discrete lifetime of 5 ps, but as seen in the traces in the near-IR region (Figure 2), apart from the fitted 1.35 ps there is no longer lifetime component and the signals decay to zero within 5 ps.

Spirilloxanthin in the LH1 Complex of Rs. rubrum. The ground-state absorption of spirilloxanthin in the LH1 complex is red-shifted compared to that in solution, with the lowest vibronic peak of the S_2 state appearing at 546 nm (Figure 1). The absorption bands of BChl appear further to the red, at 590 nm (Q_x) and 880 nm (Q_y). The excitation pulses were tuned to 540 nm to selectively excite spirilloxanthin to the lowest vibrational level of the S_2 state. Kinetic traces were measured over a broad spectral region, from 880 to 1720 nm. Representative traces are shown in Figure 4.

The energy transfer to BChl that takes place in the LH1 complex after excitation of spirilloxanthin makes the near-IR spectra considerably more complicated than those measured in solution, as the excited BChl gives rise to significant contributions in that region (ref *18*, Figure 4). The traces measured up to 950 nm contain a large negative signal that originates from the BChl bleaching and stimulated emission (SE) band that appears exclusively as a result of energy transfer from the spirilloxanthin S_2 state to the BChl Q_x state, since the direct excitation of BChl by the 540 nm excitation pulses is negligible.[32] As seen in the kinetics in Figure 4, the signal exhibits multiexponential decay. Only the earlier components can be ascribed to the decay of the excited singlet states of spirilloxanthin, as they are completely depopulated within 10 ps.[6] On time scales of tens to hundreds of picoseconds, we observe a significant loss of signal which cannot be due to the natural decay of the Q_y level of BChl, because its lifetime is ~700 ps.[33] We ascribe the observed loss exclusively to BChl dynamics which are separated from spirilloxanthin. The decay can be attributed to the annihilation of excitations among LH1 rings that are highly aggregated because of the low detergent concentration.[34] Other processes occurring on the LH1 complexes such as equilibration among BChls and vibrational relaxation of BChl can be excluded, as they occur on faster time scales and would manifest as spectral changes whereas what we observe is a loss of electronic excitations.

Simultaneous fitting of all kinetics reveals the presence of four exponential decay constants (<100 fs, 1.4 ps, 16 ps, and 160 ps), of which the first two correspond to time scales characteristic of the dynamics of the excited singlet states of spirilloxanthin.[6] The slower decays are apparently due to long-range inter-ring annihilation, and should therefore be viewed rather as effective time constants, since annihilation is not an exponential process.[34] To separate the contribution of the different processes that follow excitation to S_2, we have applied a branched global analysis modeling scheme, similar to the one that has been successful in describing the relaxation dynamics in the LH1 complex of *Rs. rubrum* in the visible region.[6] According to that scheme, the S_2 state relaxes via three separated, parallel pathways, two involving the IC to S_1 and S* and one the EET to BChl. In the analysis of the current data though, including the pathway to S* is superfluous, because in the 880−1700 nm spectral region we do not observe a 5 ps lifetime or a spectral feature that could be attributed to it. We have therefore omitted the S_2-S^* pathway from the model so that S_2 relaxes in parallel via two channels, one toward S_1 and one toward BChl, with the latter decaying biexponentially. The respective SADS resulting from this branched model are shown in Figure 5. The modification of the model has no effect on the spectral shape of the resulting S_1 SADS, which we will use to calculate the S_1 energy, because a 5 ps component included in the model to accommodate S* would carry no amplitude. This adaptation of the model only affects the relative amplitudes of the S_1 and BChl SADS, reflecting their production yields.

Upon excitation, a broad SADS appears above 950 nm (Figure 5A), peaking around 1200 nm and decaying within 100 fs (instrument response-limited). The decay of this SADS denotes the loss of ESA over the entire spectral range and the rise of strong SE at the shorter wavelengths, pointing out the depopulation of the S_2 state of spirilloxanthin and the occurrence of energy transfer to BChl. The SADS that is associated with the 1.4 ± 0.2 ps lifetime has a significantly lower amplitude (Figure 5B). Its lifetime is similar to that found for S_1 in LH1 by probing in the visible region,[6] showing that this SADS describes the S_1 state of spirilloxanthin, which in the absence of EET to BChl decays with the same time constant as in solution. The position of the S_1-S_2 absorption bands can be determined from the structure of this SADS, and the S_1 energy can be estimated. The second relaxation pathway from S_2 includes the third and fourth SADS (Figure 5C,D) which are rather flat and featureless and have decay lifetimes of 16 and 160 ps. These SADS are markedly different from the SADS of S_1 (Figure 5B), showing that they originate from a different excited species, which has been separated spectrally by the target

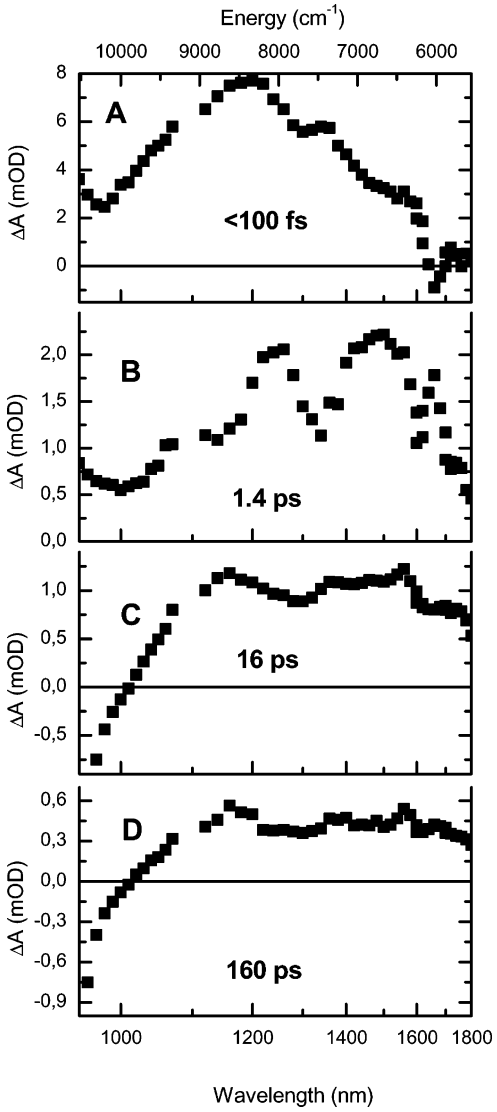

Figure 5. Target analysis SADS and associated lifetimes characterizing the spectral evolution of the transient absorption of the LH1 complex of *Rs. rubrum* in the near-IR region after excitation at 540 nm. The model assumes the parallel relaxation of S_2 via two independent channels, S_1 and BChl, with the latter having a multiexponential decay. A mild two-point smoothing has been performed to decrease the noise.

analysis. The third and fourth SADS have a spectral shape similar to that observed for the ESA of BChl in the near-IR region,[18] confirming the assignment of these SADS exclusively to BChl, which is expected to exhibit annihilation dynamics in this temporal window.

Discussion

Origin of the 1200 nm ESA Band. Upon excitation of spirilloxanthin, both in solution and in the LH1 complex, an intense ESA band appears instantly at ~1200 nm and decays with a lifetime of <100 fs. Due to the limited time resolution, this time constant cannot be determined more accurately from these measurements. This short lifetime is in good agreement with fluorescence upconversion measurements on spirilloxanthin that have shown that the lifetime of the emissive state is 60 fs.[35] Since the steady-state S_2 fluorescence spectrum of spirilloxanthin is a mirror image of the ground-state absorption spectrum[36] with a small Stokes shift of ~250 cm^{-1}, it is clear that the emissive state is the $1B_u^+$ state, leading to the conclusion that the 1200 nm ESA band is due to a transition from the excited $1B_u^+$ state. To account for the high intensity of this ESA band, the transition must be strongly allowed, leading to an assignment that the final state must be of A_g^- symmetry. This conclusion contradicts recent suggestions that some ESA bands in the near-IR region rather originate from either $1B_u^-$ or $3A_g^-$ states,[4,5] which are populated by ultrafast (~10 fs) relaxation of the initially excited $1B_u^+$ state. To support our conclusion, we can estimate the energy of a transition originating from the $1B_u^-$ state. To achieve a strongly allowed transition, the final state should have A_g^+ symmetry, and the lowest A_g^+ state of spirilloxanthin is a *cis* state, corresponding to the peak located at 380 nm (26 320 cm^{-1}). Using a spirilloxanthin $1B_u^-$ energy of 13 330 cm^{-1}, as suggested by the resonance Raman profile,[37] the energy gap between the $1B_u^-$ and $1A_g^+$ states is approximately 12 990 cm^{-1}. Such a transition would be located at 770 nm, which is clearly far off the observed ESA band at 1200 nm. A similar approach can be used to show that the 1200 nm ESA band cannot be due to a transition from the $3A_g^-$ state. The energy of the spirilloxanthin $3A_g^-$ state was determined[37] to be 14 560 cm^{-1}, and to account for a strong ESA from this state, the final state must have B_u^+ symmetry; thus, it should be observed also in the ground-state absorption spectrum at around 22 900 cm^{-1} (435 nm). However, the absorption spectrum of spirilloxanthin contains no distinct bands in this spectral region, again confirming our conclusion that the 1200 nm ESA band is indeed due to a transition originating from the initially excited $1B_u^+$ state, which decays in less than 100 fs to populate the S_1 and the S* states. The differences between our results and the data reported recently by Fujii *et al.*[4] can be partially due to our limited time resolution. However, although we may not be able to follow spectral evolution faster than 100 fs, we should observe response-limited bands below 1000 nm, which is obviously not the case (see Figures 3 and 5). It is worth pointing out that our experimental conditions were different from those in ref *4*: the transient signal at 950 nm is in our case ~35 times lower in magnitude (950-nm trace in Figure 2) than that in ref *4*. This indicates that the excitation intensities were significantly different, which may be the reason for the different results. Therefore, until the effects of high excitation intensities on the observed signals are clarified and further substantial evidence concerning the involvement of the $3A_g^-$ state is presented, we use the generally accepted picture of the S_2-S_1 IC process.

Energy of the S_1 State of Spirilloxanthin. Near-IR transient absorption spectroscopy is a technique that involves only the allowed absorption from S_1 to S_2 and probes all the possible conformations or sublevels of S_1. Furthermore, it is also applicable to carotenoids of extended conjugation. This is an advantage over the direct measurement of fluorescence for the detection of the dark states of carotenoids in solution. Fluorescence measurements[36] become rather ambiguous when applied to longer carotenoids, such as spirilloxanthin, because they involve the direct detection of very small signals originating from the symmetry-forbidden emission of short-lived states. Resonance Raman excitation profiles have also been used to detect the S_1 and other carotenoid states and for determining their energies.[38] Indirect estimation of the energy of the S_1 state is possible by application of the energy gap law, which relates the energy of a state to its lifetime. As demonstrated by Frank *et al.*,[9] after the S_1 lifetime of a series of spheroidene analogues with conjugation lengths varying from 7 to 13 double bonds was measured, it was possible to extrapolate the S_1 energies for the longer carotenoids by using the S_1 energies of the shorter

ones determined by fluorescence measurements. Two-photon absorption spectroscopy is the only method apart from near-IR transient absorption that has been applied in the study of the S_1 state of carotenoids bound to LH complexes,[39] but as it probes the BChl fluorescence, it yields only excitation spectra of carotenoid S_1 states active in energy transfer, which do not necessarily portray the properties of all configurations present in the system being studied.[40]

Spirilloxanthin in Solution. The aforementioned different approaches for determination of the energy of the S_1 state of carotenoids in solution have yielded considerably different values. For spheroidene, the S_1 energy reported by Polivka *et al.*[17] is 13 400 cm^{-1}, while by fluorescence[41] and resonance Raman profiles,[38] it has been reported to be higher, 14 200 cm^{-1}. Application of the energy gap law[9] has also resulted in a value of 14 200 cm^{-1}. These inconsistencies have been discussed[17] in terms of a multiple-conformer model, which proposed that fluorescence originates preferably from specific conformers or subpopulations of the S_1 state that are not the lowest in energy. Spirilloxanthin is a carotenoid that is known to isomerize spontaneously to a significant extent, forming a large number of different conformers on a time scale of minutes.[26,27] Consequently, it is important to consider the possible mixtures of *all-trans* and other various conformers when discussing its excited-state properties. The S_2 energy of *all-trans*-spirilloxanthin in *n*-hexane is ~19 010 cm^{-1} (absorption peak at 526 nm), while the distorted conformers have a higher S_2 energy.[26−28] Because of the lengthy nature of the measurements that we have performed on spirilloxanthin, measuring on a mixture of isomers was inevitable. The absorption spectrum (Figure 1) shows that the lowest S_2 transition is located at 522 nm, 4 nm to the blue compared to that of the *all-trans* species, implying that a certain amount of molecules are in a twisted conformation, which can have a shift in their S_0-S_2 energy[27] of up to 450 cm^{-1}. It is uncertain to what extent the conformation plays a role in the energy of the S_1 state, but it is likely that the energy of S_1 is shifted in a manner similar to that of S_2. In the work on the S_1 state of spheroidene,[17] it has been asserted that the carotenoid can exist in different conformations while in the S_1 excited state, which leads to a broadening of the S_1-S_2 absorption band. Since spirilloxanthin can already be distorted in the ground state, it seems logical that the effect on the S_1 state will be larger.

Knowledge of the energies of the S_0-S_2 and S_1-S_2 transitions is a prerequisite for the determination of the energy of S_1 when applying the near-IR transient absorption technique. The presence of isomers complicates this process, as the different conformers make slightly different contributions to the IR spectrum, leading to the broadening of the bands, and especially of the lower-energy one. Assuming the same situation as for spheroidene, the 0−0 band is expected to be more intense and narrower than the higher vibrational bands that are broadened due to a mixing of C−C and C═C stretching modes. Nevertheless, as seen in the SADS (Figure 3B) of the S_1-S_2 ESA, this is not the case, as the 0−0 band is clearly broader and approximately the same in intensity as the 0−1 band. The width of the 0−0 band is on the order of 1200 ± 100 cm^{-1}, which when compared to the width of the corresponding band in spheroidene (750 cm^{-1})[17] does suggest the existence of multiple conformers in the S_1 state. In addition, the lack of an additional sub-picosecond component due to the vibrational relaxation of the S_1 state[17,30,31] might indicate that transitions from vibrationally hot forms of the S_1 state also contribute to the spectrum during the S_1-S_0 relaxation, leading to a further broadening of the 0−0 vibrational band of the S_1-S_2 spectral profile.

If we assume that different species make distinct contributions to the S_1-S_2 ESA spectrum, we can fit the S_1-S_2 SADS with Gaussian bands. At least two distinct spectral components are needed to fit the 0−0 feature, corresponding to different conformations in the S_1 state. The S_1 states of different conformers are not expected to have markedly distinct lifetimes, as shown for *all-trans*- and locked *cis*-spheroidene.[42] Therefore, the only constraints that can be applied in the fitting concern the widths and positions of the bands. A plausible solution is reached when one band is located around 7600 cm^{-1} and a second one around 7150 cm^{-1}, demonstrating the extent of the broadening of the 0−0 band. We note that this fit is not unique. However, the higher-energy band, which is likely to correspond to the *all-trans* form as it has the larger S_1-S_2 gap,[17] is always located around 7600 ± 100 cm^{-1}. The ambiguity is increased for the twisted conformers, which are most likely to contribute a number of components on the red side of the band, and consequently, it seems obvious that the fitting of this broad distribution cannot produce a unique result.

By using the 19 160 cm^{-1} energy for S_0-S_2 transition of our spirilloxanthin mixture of conformers, we calculate the S_1 energy to be 11 560 ± 200 cm^{-1}. The S_2 energy of pure *all-trans*-spirilloxanthin is 150 cm^{-1} lower than the value observed in these experiments for a mixture of isomers. If we assume a similar shift for the S_1 energy, the estimated value of 11 560 cm^{-1} should be considered the upper limit for the S_1 energy of *all-trans*-spirilloxanthin, with a more realistic value ~100 cm^{-1} lower, around 11 450 ± 200 cm^{-1}. On the other hand, determining the S_1 energy of the twisted forms is not as straightforward; they contribute to the red side of the S_1-S_2 spectrum and to the blue side of the ground-state absorption, with an S_2 energy shift that reaches 450 cm^{-1} compared to those of *all-trans*-spirilloxanthin.[27] As mentioned already, we estimate that they will accordingly have S_1 energies higher than that of *all-trans*-spirilloxanthin. Considering an upper limit of 19 500 cm^{-1} for the S_2 energy of the twisted species and a corresponding minimal S_1-S_2 gap of 7150 cm^{-1}, their S_1 energies are likely to be distributed up to 12 200 ± 200 cm^{-1}. The value of 11 900 cm^{-1} that has been estimated for the spirilloxanthin S_1 state by fluorescence measurements[36] indicates that the fluorescence might indeed originate from conformers other than *all-trans* species, as was already proposed for spheroidene.[17] Application of the energy gap law to a 13-double bond analogue of spheroidene[9] has led to a value of 11 775 cm^{-1}, which lies between the values estimated for spirilloxanthin by near-IR spectroscopy and by fluorescence measurements. However, since the studied spheroidene analogue is structurally different from spirilloxanthin and has a shorter S_1 lifetime, 1.1 ps, a direct comparison may not be reliable.

Spirilloxanthin in LH1. Near-IR transient absorption and two-photon excitation are the only methods developed so far that can measure the energy of the S_1 state of carotenoids embedded in LH proteins. For LH complexes, as in solution, the results are contradictory, since the near-IR transient absorption method[18] gives an S_1 energy for spheroidene of 13 400 cm^{-1} while two-photon excitation[39] locates it higher, at 13 900 cm^{-1}. However, the higher energy found in the latter case can be attributed to significant EET occurring from the vibrationally hot forms of the S_1 state of spheroidene to BChl.[7] It is known that in the LH1 complex the carotenoid is spatially confined and cannot twist freely due to the protein scaffold, as demonstrated for rhodopin glucoside in the LH2 complex of *Rhodopseudomonas*

acidophila.[18] Although confinement in the protein environment causes some deviation from an ideal *all-trans* conformation, the presence of *cis* isomers can safely be ruled out. Therefore, the measurements on the LH1 complex are important for determining the energy of the S_1 state of *all-trans*-spirilloxanthin, as it is expected to be similar to that in solution, as shown already for the S_1 energy of spheroidene and rhodopin glucoside, which in their native LH2 complexes does not differ from that in solution.[18]

The second SADS in the measurements on spirilloxanthin in the LH1 complex (Figure 5B) has a lifetime of 1.4 ps and reflects the S_1-S_2 transition. This SADS displays two distinct peaks located around 6770 (0−0) and 8070 cm^{-1} (0−1), with their energy gap of 1300 cm^{-1} matching the spacing of the two lowest vibrational bands of the S_0-S_2 transition of spirilloxanthin in the LH1 complex (1270 cm^{-1}). The third peak of the S_1-S_2 absorption is not well-resolved, most probably due to the strong BChl signal at shorter wavelengths that interferes with the S_1-S_2 ESA.[18] Notably, the 0−0 peak has a width of 1000 ± 100 cm^{-1}, and is thus narrower than the corresponding transition in solution, indicating the effect of spatial confinement of spirilloxanthin when bound to the LH1 complex. The fact that the 0−0 peak is still broader than that of spheroidene both in solution and in the LH2 complex[17,18] supports the idea that during the S_1-S_0 relaxation some higher vibrational levels of the S_1 state remain populated, as was also proposed for β-carotene.[43] Having assigned the 0−0 band of the S_1-S_2 transition of spirilloxanthin in the LH1 complex, we can calculate the energy of S_1 to be $18\,300 - 6770$ cm^{-1} (=11 530 $\pm$ 200 cm^{-1}). This value is very close to the value that we obtained for *all-trans*-spirilloxanthin in *n*-hexane, providing yet another piece of evidence that the energy of the S_1 state of *all-trans*-spirilloxanthin is approximately 11 500 cm^{-1}.

Knowing the S_1 energy of spirilloxanthin, we can consider its effect on the EET efficiency to BChl in the LH1 complex of *Rs. rubrum*. The lowest energy level of BChl in LH1 is the Q_y band at 11 330 cm^{-1}, very close to the energy of S_1 as estimated above. The S_1 emission maximum of carotenoids corresponds to the 0−2 vibrational transition,[44] thus making the spectral overlap between the S_1 emission and the B880 Q_y absorption negligible and energy transfer unfavorable. In addition to the poor overlap, the short lifetime of the S_1 state in spirilloxanthin makes S_1-BChl EET even more unlikely. Calculations for carotenoid−BChl energy transfer in LH2 complexes, where the lowest acceptor states lie at around 11 700 cm^{-1}, have also shown that for S_1 energies lower than 13 000 cm^{-1} the transfer rate is very slow.[45] Although the acceptor states in the system studied here are located ~400 cm^{-1} lower, the absence of S_1 energy transfer is in good agreement with the calculations on the LH2 system, as the value of 11 500 cm^{-1} determined for the S_1 state of spirilloxanthin is far beyond the limits of efficient energy transfer predicted by calculations.

Interestingly, no features that could be related to a state other than S_1 are observed in our measurements, even though the S* state has a distinct temporal behavior and a clear spectral signature in the visible region both in solution and in the LH1 complex.[6] The fact that we do not see any 5 ps component that can be attributed to the decay of the S* state of spirilloxanthin must be due to a shift of the S* potential surface leading to a significant decrease in the Franck−Condon factors between the S* and S_2 states. In this case, there is no final state to observe ESA from S* in this spectral region. Furthermore, in the LH1 complex, the large SE of BChl, which is red-shifted compared to that of BChl in the LH2 complex, might be masking the possible transient spectrum of a radical similar to that observed in LH2.[18] On the other hand, it is possible that the generation of the radical is not connected to the formation of S*, as initially proposed,[18] but rather to the structure of the LH protein, which differs in the LH1 and LH2 complexes. In any case, our data provide no indications of a connection between the S* and the carotenoid radical. Similarly, we have not observed any spectral features in the near-IR region that can be attributed to the triplet state of spirilloxanthin, which is formed with a high yield via S* within picoseconds after direct excitation.[6] Although signals due to the T_1-T_2 transition were detected in the near-IR region for carotenoids in solution,[46] given the fact that these signals are significantly weaker than those of the T_1-T_n transition in the visible region, the T_1-T_2 ESA is obviously hidden under the distinct BChl ESA that covers the entire region.

Conclusions

Probing the absorption changes in the near-IR region after selective excitation of spirilloxanthin to its S_2 state, both in *n*-hexane and in the LH1 complex of *Rs. rubrum*, has enabled us to obtain and study the spectral profile of the S_1-S_2 transition. *All-trans*-Spirilloxanthin has its S_1 state around 11 500 cm^{-1}, both in solution and in the LH1 complex. The low energy transfer efficiency from spirilloxanthin to BChl is thus explained as a consequence of the S_1 state being incapable of transferring energy to the B880 band, implying that the S_2 state mediates the energy transfer to BChl in the LH1 complex with 30% efficiency. We have also presented the spectral and temporal profile of an intense broad absorption band that appears upon excitation to S_2 and is short-lived, signifying the ultrafast IC process from the S_2 to the S_1 state. Finally, we have not observed any features of the S* state or a spirilloxanthin radical in our measurements; thus, elucidation of the properties of these states and their possible relation will be the target of our future studies.

Acknowledgment. E.P. thanks the European Science Foundation's Program on Femtochemistry and Femtobiology (ULTRA) for supporting his visit to Lund. The work at Lund University was performed with funding from the Swedish Research Council, the Wallenberg Foundation, and the Crafoord Foundation. T.P. thanks DESS (Delegationen för Energiförsörjning i Sydsverige) for financial support. We also thank J. Henderson for assistance with carotenoid preparation.

References and Notes

(1) Frank, H. A.; Cogdell, R. J. *Photochem. Photobiol*. **1996**, *63*, 257.
(2) Ritz, T.; Damjanovic, A.; Schulten, K.; Zhang, J. P.; Koyama, Y. *Photosynth. Res.* **2000**, *66*, 125.
(3) Tavan, P.; Schulten, K. *J. Chem. Phys.* **1986**, *85*, 6602.
(4) Fujii, R.; Inaba, T.; Watanabe, Y.; Koyama, Y.; Zhang, J. P. *Chem. Phys. Lett.* **2003**, *369*, 165.
(5) Cerullo, G.; Polli, D.; Lanzani, G.; De Silvestri, S.; Hashimoto, H.; Cogdell, R. J. *Science* **2002**, *298*, 2395.
(6) Gradinaru, C. C.; Kennis, J. T. M.; Papagiannakis, E.; van Stokkum, I. H. M.; Cogdell, R. J.; Fleming, G. R.; Niederman, R. A.; van Grondelle, R. *Proc. Natl. Acad. Sci. U.S.A.* **2001**, *98*, 2364.
(7) Papagiannakis, E.; Kennis, J. T. M.; van Stokkum, I. H. M.; Cogdell, R. J.; van Grondelle, R. *Proc. Natl. Acad. Sci. U.S.A.* **2002**, *99*, 6017.
(8) Papagiannakis, E.; Das, S. K.; Gall, A.; van Stokkum, I. H. M.; Robert, B.; van Grondelle, R.; Frank, H. A.; Kennis, J. T. M. *J. Phys. Chem. B* **2003**, *107*, 5642.
(9) Frank, H. A.; Desamero, R. Z. B.; Chynwat, V.; Gebhard, R.; vanderHoef, I.; Jansen, F. J.; Lugtenburg, J.; Gosztola, D.; Wasielewski, M. R. *J. Phys. Chem. A* **1997**, *101*, 149.
(10) Chynwat, V.; Frank, H. A. *Chem. Phys.* **1995**, *194*, 237.
(11) Zhang, J. P.; Fujii, R.; Qian, P.; Inaba, T.; Mizoguchi, T.; Koyama, Y.; Onaka, K.; Watanabe, Y.; Nagae, H. *J. Phys. Chem. B* **2000**, *104*, 3683.
(12) Picorel, R.; Bélanger, G.; Gingras, G. *Biochemistry* **1983**, *22*, 2491.
(13) Karrasch, S.; Bullough, P. A.; Ghosh, R. *EMBO J.* **1995**, *14*, 631.

(14) Duysens, L. N. M. Ph.D. Thesis, University of Utrecht, Utrecht, The Netherlands, 1952.
(15) Papagiannakis, E. Manuscript in preparation, 2003.
(16) Polivka, T.; Herek, J. L.; Zigmantas, D.; Akerlund, H. E.; Sundstrom, V. *Proc. Natl. Acad. Sci. U.S.A.* **1999**, *96*, 4914.
(17) Polivka, T.; Zigmantas, D.; Frank, H. A.; Bautista, J. A.; Herek, J. L.; Koyama, Y.; Fujii, R.; Sundstrom, V. *J. Phys. Chem. B* **2001**, *105*, 1072.
(18) Polivka, T.; Zigmantas, D.; Herek, J. L.; He, Z.; Pascher, T.; Pullerits, T.; Cogdell, R. J.; Frank, H. A.; Sundstrom, V. *J. Phys. Chem. B* **2002**, *106*, 11016.
(19) Polivka, T.; Zigmantas, D.; Sundstrom, V.; Formaggio, E.; Cinque, G.; Bassi, R. *Biochemistry* **2002**, *41*, 439.
(20) Zigmantas, D.; Hiller, R. G.; Sundstrom, V.; Polivka, T. *Proc. Natl. Acad. Sci. U.S.A.* **2002**, *99*, 16760.
(21) van Niel, C. B.; Goodwin, T. W.; Sissins, M. E. *Biochem. J.* **1956**, *63*, 408.
(22) Komori, M.; Ghosh, R.; Takaichi, S.; Hu, Y.; Mizoguchi, T.; Koyama, Y.; Kuki, M. *Biochemistry* **1998**, *37*, 8987.
(23) van Stokkum, I. H. M.; Scherer, T.; Brouwer, A. M.; Verhoeven, J. W. *J. Phys. Chem.* **1994**, *98*, 852.
(24) Holzwarth, A. R. In *Biophysical Techniques in Photosynthesis*; Amesz, J., Hoff, A. J., Eds.; Kluwer: Dordrecht, The Netherlands, 1996; p 75.
(25) Britton, G. In *Carotenoids*; Britton, G., Liaaen-Jensen, S., Pfander, H., Eds.; Birkhäuser: Basel, Switzerland, 1995; Vol. 1B (Spectroscopy), p 13.
(26) Polgar, A.; van Niel, C. B.; Zechmeister, L. *Arch. Biochem.* **1944**, *5*, 243.
(27) Lindal, T.-R.; Liaaen-Jensen, S. *Acta Chem. Scand.* **1997**, *51*, 1128.
(28) Koyama, Y.; Takatsuka, I.; Kanaji, M.; Tomimoto, K.; Kito, M.; Shimamura, T.; Yamashita, J.; Saiki, K.; Tsukida, K. *Photochem. Photobiol.* **1990**, *51*, 119.
(29) Zhang, J. P.; Skibsted, L. H.; Fujii, R.; Koyama, Y. *Photochem. Photobiol.* **2001**, *73*, 219.
(30) de Weerd, F. L.; van Stokkum, I. H. M.; van Grondelle, R. *Chem. Phys. Lett.* **2002**, *354*, 38.
(31) Billsten, H. H.; Zigmantas, D.; Sundstrom, V.; Polivka, T. *Chem. Phys. Lett.* **2002**, *355*, 465.
(32) Gradinaru, C. C. Ph.D. Thesis, Vrije Universiteit, Amsterdam, The Netherlands, 2001.
(33) Monshouwer, R.; Abrahamsson, M.; van Mourik, F.; van Grondelle, R. *J. Phys. Chem. B* **1997**, *101*, 7241.
(34) van Grondelle, R. *Biochim. Biophys. Acta* **1985**, *811*, 147.
(35) Kennis, J. T. M. Unpublished results.
(36) Fujii, R.; Ishikawa, T.; Koyama, Y.; Taguchi, M.; Isobe, Y.; Nagae, H.; Watanabe, Y. *J. Phys. Chem. A* **2001**, *105*, 5348.
(37) Furuichi, K.; Sashima, T.; Koyama, Y. *Chem. Phys. Lett.* **2002**, *356*, 547.
(38) Sashima, T.; Shiba, M.; Hashimoto, H.; Nagae, H.; Koyama, Y. *Chem. Phys. Lett.* **1998**, *290*, 36.
(39) Krueger, B. P.; Yom, J.; Walla, P. J.; Fleming, G. R. *Chem. Phys. Lett.* **1999**, *310*, 57.
(40) Walla, P. J.; Linden, P. A.; Ohta, K.; Fleming, G. R. *J. Phys. Chem. A* **2002**, *106*, 1909.
(41) Fujii, R.; Onaka, K.; Kuki, M.; Koyama, Y.; Watanabe, Y. *Chem. Phys. Lett.* **1998**, *288*, 847.
(42) Bautista, J. A.; Chynwat, V.; Cua, A.; Jansen, F. J.; Lugtenburg, J.; Gosztola, D.; Wasielewski, M. R.; Frank, H. A. *Photosynth. Res.* **1998**, *55*, 49.
(43) Yoshizawa, M.; Aoki, H.; Hashimoto, H. *Phys. Rev. B* **2001**, *6318*.
(44) Frank, H. A.; Bautista, J. A.; Josue, J. S.; Young, A. J. *Biochemistry* **2000**, *39*, 2831.
(45) Hsu, C. P.; Walla, P. J.; Head-Gordon, M.; Fleming, G. R. *J. Phys. Chem. B* **2001**, *105*, 11016.
(46) Bachilo, S. M. *J. Photochem. Photobiol., A* **1995**, *91*, 111.